Jonathan P, PH Taylor, PA Tromans, Storm waves in the northern North Sea, BOSS '94, 7th Intl Conf on the Behaviour of Offshore Structures; 12-15 July 1994; Massachusetts, USA, Proc Publ by Pergamon, ISBN 0 08 041914 3, Vol 2, p.481, 14p, 15 ref, 1tab, 9 fig

STORM WAVES IN THE NORTHERN NORTH SEA

P. Jonathan, P.H. Taylor and P.S. Tromans

Shell Research Rijswijk, The Netherlands.

ABSTRACT

Offshore measurements have been made at the Tern platform in the northern North Sea during three severe winter storms. Surface spectra for all three storms are similar, all showing an ω^{-4} tail. The wave fields are directionally spread with lowest spreading at a frequency below the spectral peak. After adjustment for 2nd order nonlinearity, the largest crests and troughs are Rayleigh distributed and the most probable shape for an extreme crest or trough is close to the correlation function for surface elevation. This supports the idea of a design wave for use in the design or reliability assessment of offshore structures.

KEYWORDS

Waves, storms, directional spreading, Rayleigh, North Sea, correlation.

INTRODUCTION

Safe and cost-effective production of oil offshore requires methods for assessing the reliability of offshore structures. The computation of wave forces on offshore structures requires accurate knowledge of the ocean environment as well as the mechanisms of fluid loading. In order to obtain information on both of these issues, the Tern platform in the northern North Sea was instrumented. Tern is located northeast of the Shetland Islands, between Scotland and Norway, in 167m of water. The structure consists of a piled steel jacket supporting the topside facilities. The monitoring system on Tern consists of strain gauges positioned near the base of the four corner legs, a wind sensor placed on top of the derrick, two wave-height sensors at different locations, and two water-particle velocity meters attached to the jacket at -41m. These velocity meters record flow in two orthogonal horizontal directions.

The specific objective of the measurement system was to allow simultaneous recording of the environmental conditions and the platform's global storm loading. Thus, the Tern monitoring program provides an opportunity to further validate models of both the ocean environment and the global forces exerted on an offshore platform. This paper will discuss oceanographic data obtained during winter storms in 1992 and 1993. Figure 1 shows the plan of the structure with the velocity meters, surface elevation sensors and the main wave attack directions for the

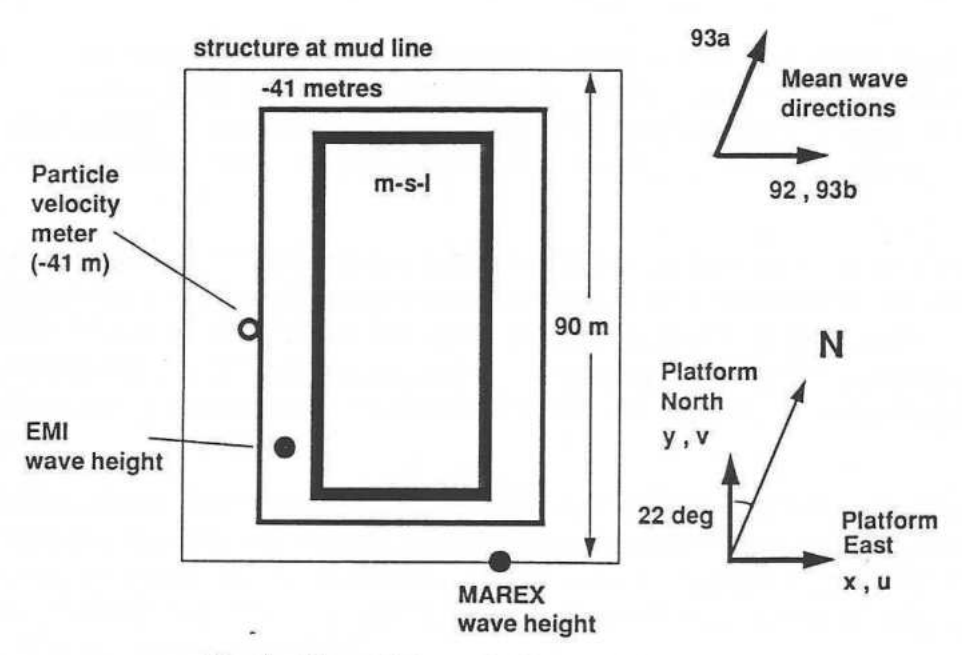


Fig. 1. Plan of Tern platform and instrumentation.

| 1992 | | | | | | |
|---------|---------|------|------|-----------|---------|-----------|
| Date in | Hour of | | | Mean | Mean | Mean |
| January | day | Hs | Tp | wave | current | current |
| | | (m) | (s) | direction | (m/s) | direction |
| 1 | 2 | 8.9 | 13 | 217 | 0.188 | 205.2 |
| 1 | 3 | 10.8 | 14 | 188 | 0.27 | 180 |
| 1 | 6 | 13.8 | 15 | 169 | 0.368 | 137.2 |
| 1 | 7 | 12.5 | 15 | 163 | 0.41 | 124.08 |
| 1 | 8 | 11.3 | 15 | 164 | 0.336 | 112.75 |
| _1 | 11 | 9.3 | 12.5 | 161 | 0.022 | 116.57 |
| 1993a | | | | | | |
| Date in | Hour of | | | Mean | Mean | Mean |
| January | day | Hs | Tp | wave | current | current |
| | | (m) | (s) | direction | (m/s) | direction |
| 3 | 23 | 11.1 | 13.5 | 253 | 0.13 | 180 |
| 4 | 0 | 12.2 | 13.5 | 252 | 0.141 | 188.13 |
| 4 | 1 | 12.4 | 12.5 | 254 | 0.17 | 180 |
| 4 | 2 | 11.2 | 14.5 | 253 | 0.163 | 169.38 |
| 4 | 3 | 11.7 | 13.5 | 253 | 0.196 | 165.26 |
| 4 | 4 | 12.7 | 14.5 | 250 | 0.193 | 158.75 |
| 4 | 5 | 12.2 | 14.5 | 248 | 0.198 | 139.09 |
| 4 | 6 | 11.5 | 14.5 | 255 | 0.191 | 132.88 |
| 4 | 7 | 11 | 14.5 | 251 | 0.197 | 120.47 |
| 1993b | | | | | | |
| Date in | Hour of | | | Mean | Mean | Mean |
| January | day | Hs | Tp | wave | current | current |
| | | (m) | (s) | direction | (m/s) | direction |
| 17 | 17 | 11.1 | 13.5 | 186 | 0.081 | 97.13 |
| 17 | 19 | 12.1 | 14 | 183 | 0.08 | 90 |
| 17 | 20 | 11.1 | 13.5 | 172 | 0.082 | 75.96 |
| 17 | 21 | 11.8 | 14.5 | 172 | 0.063 | 71.57 |
| 17 | 22 | 10.8 | 12 | 169 | 0.064 | 51.34 |
| 17 | 23 | 11.4 | 14.5 | 164 | 0.063 | 71.57 |
| 18 | 0 | 11.9 | 14.5 | 162 | 0.067 | 116.57 |
| 18 | 1 | 11.4 | 15 | 160 | 0.085 | 110.56 |

Table 1. Environmental parameters for the storms analysed.

peaks of the measured storms. Directions are measured anticlockwise from Platform East, wave directions 'from' and current directions 'to'. Table 1 shows the characteristics (as hourly averages) of the storms analysed in this paper. Only surface elevation data from the EMI laser sensor is considered here. The particle velocity meter is a Marsh-McBurney electromagnetic type.

The data analysis is divided into two sections. First we study hour-by-hour surface spectra and directional spreading including some comparisons with disc buoy measurements from a nearby location. This is done to show that spectral features, observed by Donelan et al., 1985 (at much smaller scale) in Lake Ontario and by Forristal et al., 1978 for a tropical storm, are also seen in severe winter storms in the northern North Sea. This also provides a quality control on the data.

Then we examine the properties of individual waves and wave statistics. In particular we show that both the expected time history of large peaks, and their probability of occurrence, can be predicted by models based on linear statistics with second-order corrections. The principal effects of non-linearity (trough-crest asymmetry etc.) play no significant role in modifying the local dynamics of the wave-field.

The local properties of extreme waves and their probability of occurrence are key features in Shell's approach to the design and reliability assessment of offshore structures (van de Graaf, Tromans and Efthymiou, 1994).

THE SURFACE SPECTRUM AND DIRECTIONAL SPREADING

Many measurements of wind driven waves on deep water (eg. Forristall et al., 1978; Donelan et al., 1985; Wang, 1992) have demonstrated that the high frequency tail of the surface displacement spectrum decays approximately as ω^{-4} not as ω^{-5} as is assumed for model spectra such as Pierson-Moskowitz and JONSWAP. Figure 2a shows the measured spectra for the peak hours of three large northern North Sea storms. These same spectra are replotted in the manner proposed by Donelan et al. in Fig. 2b . Each spectrum is multiplied by ω^4 and normalised by the average level of the spectral estimates in the frequency band 1.5 $\omega_p < \omega < 3$ ω_p . Note that the enhancement around the spectral peak is different for each of the storms. Donelan's results indicate that this is due to different values of the wind speed parameter (U/c_p), where U in the average wind speed in the mean wave direction and c_p is the phase speed of waves at the spectral peak.

Figure 3a shows hourly surface spectra for the growth phase of the 1992 storm and Fig. 3b shows the decay phase. The high frequency tails (above about 0.1Hz) of all of these spectra are very similar, suggesting that the ω^{-4} form for the tail and its intensity are unaltered by changes close to the spectral peak. As the storm builds up, the peak in the spectrum sharpens and is shifted to lower frequency (Fig. 3a). As the storm decays, this spectral peak frequency hardly alters at least initially.

The mean wave direction as a function of frequency can be determined from the cross-spectra for the two orthogonal velocity signals each with the surface elevation. If these cross-spectra are $(S_{\eta u}, S_{\eta v})$, then the mean wave direction (θ_0) is given by

$$tan(\theta_0) = S_{nv}/S_{nu}$$

An example of the mean wave direction as a function of frequency is shown in Fig. 4 for the storm 1993b for an hour every two hours. Over the energy containing frequency range the

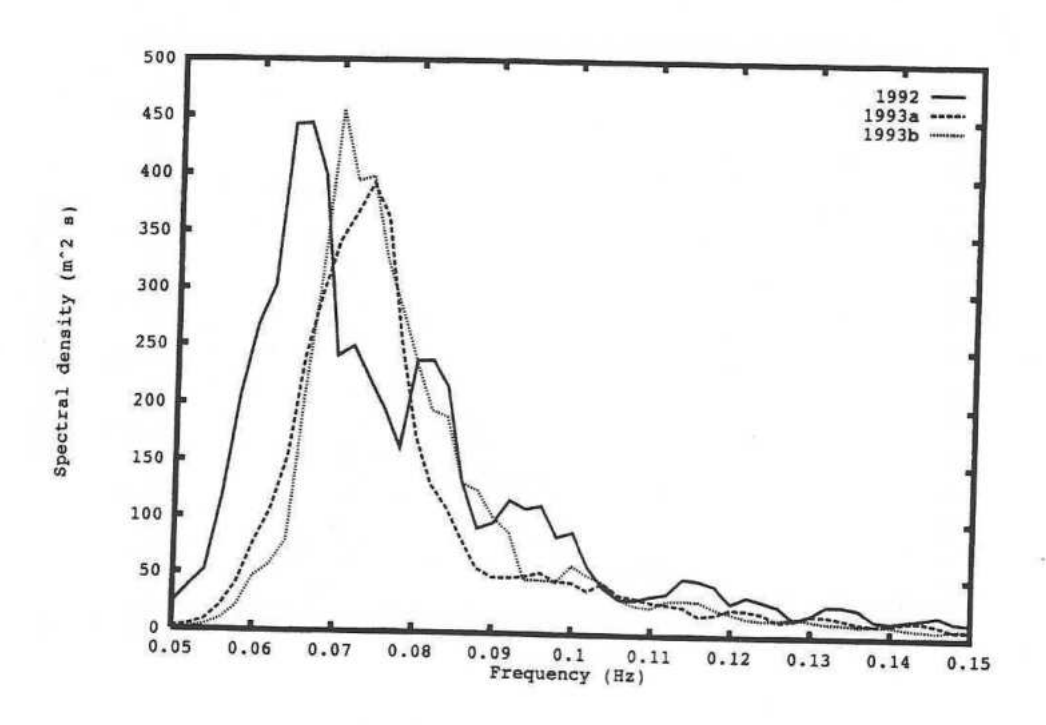


Fig. 2a. Surface spectra for the peak of each storm.

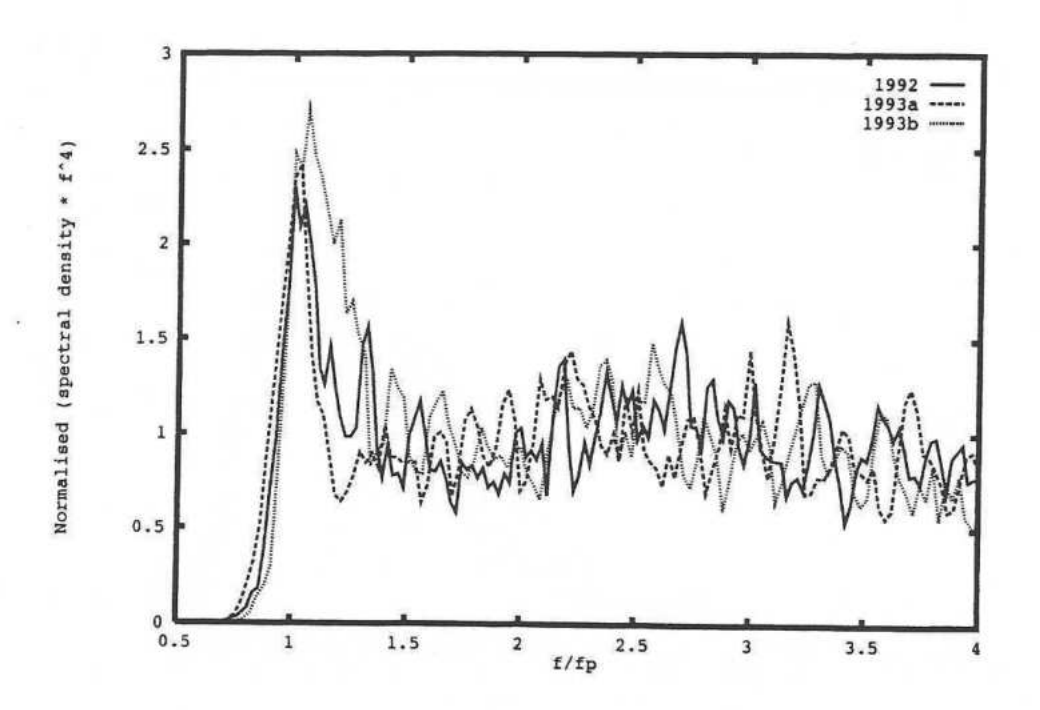


Fig. 2b. Normalised spectra $\times f^4$

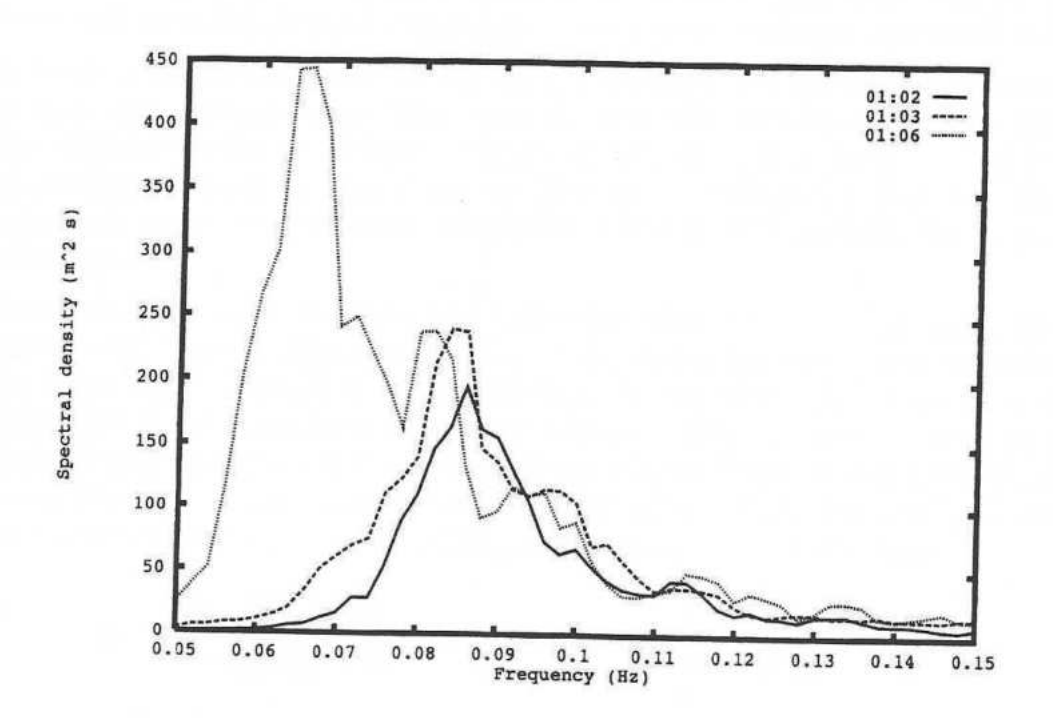


Fig. 3a. Growth of storm 1992.

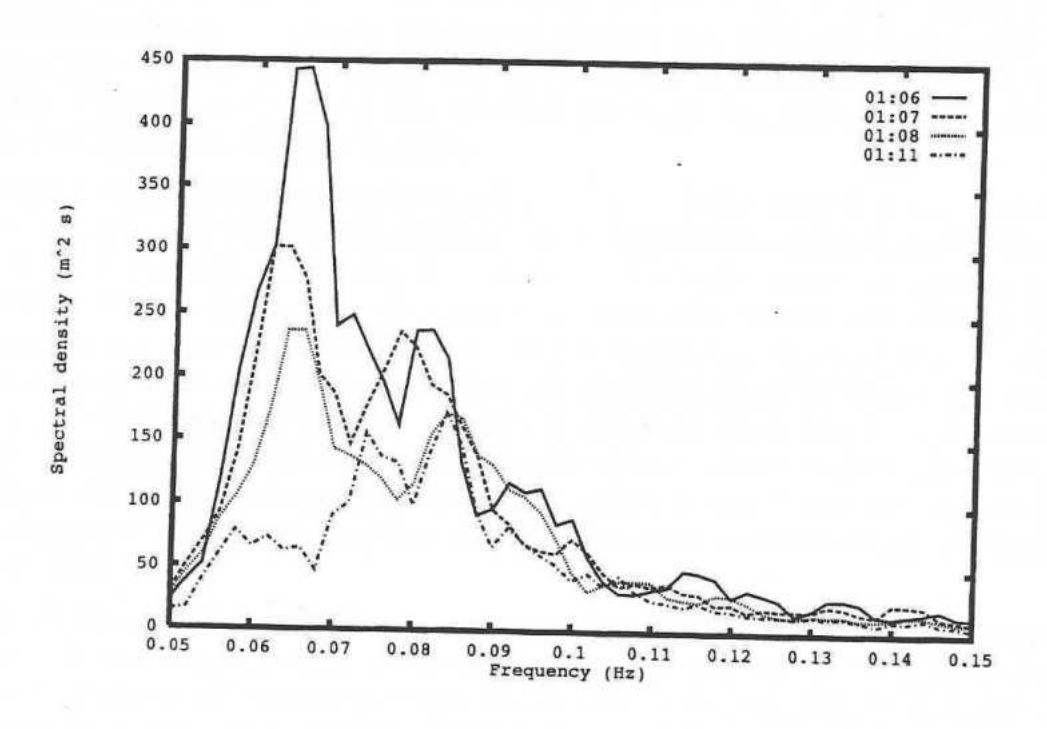


Fig. 3b. Decay of storm 1992.

mean direction for each hour is very close to uniform. However, over intervals of two hours the overall wave field is slowly rotating in response to the changing mean wind direction.

Both the mean wave direction and the average spreading are derived from the two-component velocity (u,v) measurements. The empirical probability density of velocity obtained from digitizing and binning the complete velocity vector signal for the hour 17:19 (defined in terms of the date (17), and the hour (19), see Table 1) is shown in Fig. 5 as a contour plot. The major axis is close to east-west, compatible with the 183° obtained from the ratio of the cross-spectra.

Once the mean wave direction has been established, the wave spreading remains to be investigated. The probability density (Fig. 5) shows that large transverse velocities normal to the mean wave direction do occur. Spreading is important as it leads to a reduction in kinematics in the mean wave direction and hence a reduction in global load on a structure. Spreading can be represented by a factor ϕ which is the frequency dependent reduction in the r.m.s. of horizontal kinematics compared to the value in a uni-directional sea with the same surface spectrum. This factor (ϕ) has been estimated in two different ways

$$\phi_1 = \left\{ \frac{S_{\eta u}^2 + S_{\eta v}^2}{S_{\eta \eta}(S_{uu} + S_{vv})} \right\}^{1/2} \quad \text{and} \quad \phi_2 = \left\{ \frac{S_{ViVi}}{\omega^2 \exp(-2kz) \; S_{\eta \eta}} \right\}^{1/2}$$

where $S_{\eta\eta}$ is the surface spectrum, S_{uu} and S_{vv} are the measured velocity spectra for the two orthogonal measurement directions and S_{viv} is the spectrum of the velocity vector (u,v) resolved along the mean wave direction. The frequency is ω and the associated linear wavenumber is k. The velocity meters are located at z=41 metres below mean-sea-level. These equations are derived in Forristall et al., 1981.

Both methods rely on the linear dependence between the horizontal velocity field and the vertical elevation in a uni-directional sea. Method (1) retains the correlation structure of the velocity and elevation signals, thus any spatial separation between the surface and velocity sensors would alter the results. Method (2) assumes that the in-line velocity and the surface signal would be completely correlated if they were recorded at the same physical location but makes no requirement that the measurements are made close together. It does however rely on the calibration of the velocity meters.

Results for the 1992 storm are shown in Fig. 6a. Close to the spectral peak, both methods give similar results on a frequency by frequency basis suggesting that the in-line velocity is approx. 0.9x the uni-directional velocity. For this storm the waves were moving in a west-to-east direction and the 20m horizontal separation between the surface and velocity sensors was along the wave crest direction, which should minimize any effects of separation for method (1). Although method (2) makes no use of the cross-spectra, its derivation assumes that there is no noise in the signals. This lack of tolerance of noise explains why the method breaks down away from the spectra peak where the relative noise levels are much higher. It is significant that the frequency corresponding to least spreading is well below the peak in the surface energy spectrum. A similar trend has also been observed by Donelan et al., 1985 and Forristall et al., 1981.

As a check on the data, Fig. 6b shows a comparison of the energy spectrum and spreading for 1 hour around the peak of the 1992 storm as recorded at Tern and from a disc buoy located close to the North Cormorant platform 13 km to the south east. Differences in the variation of ϕ with frequency can be interpreted at least in part in terms of differences between the measured spectra.

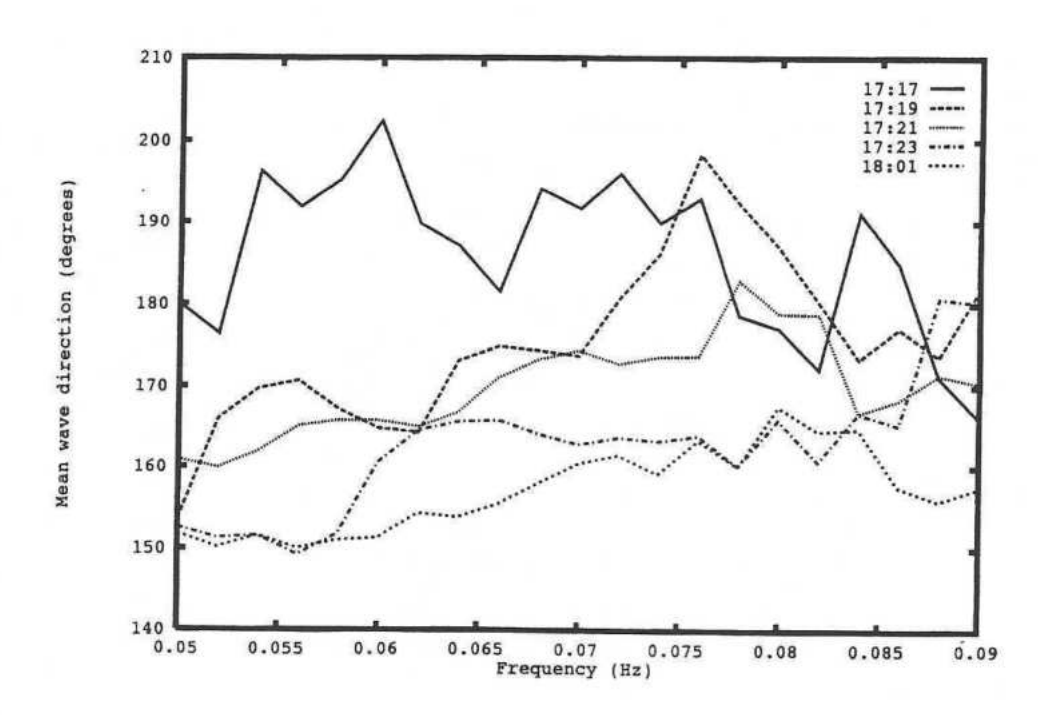


Fig. 4. Mean wave directions for storm 1993b.

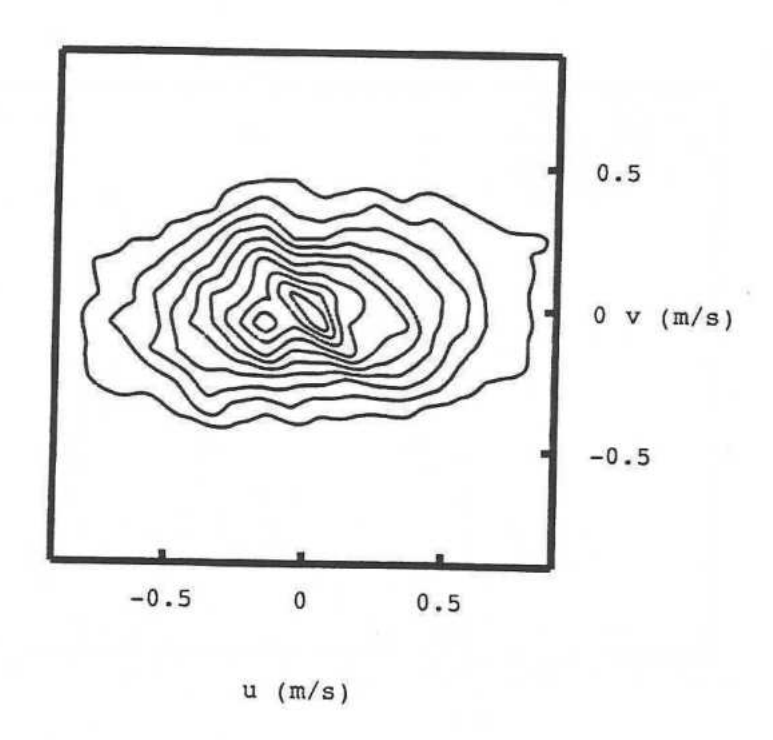


Fig. 5. Contour plot of velocity for hour 17:19 of storm 1993b.

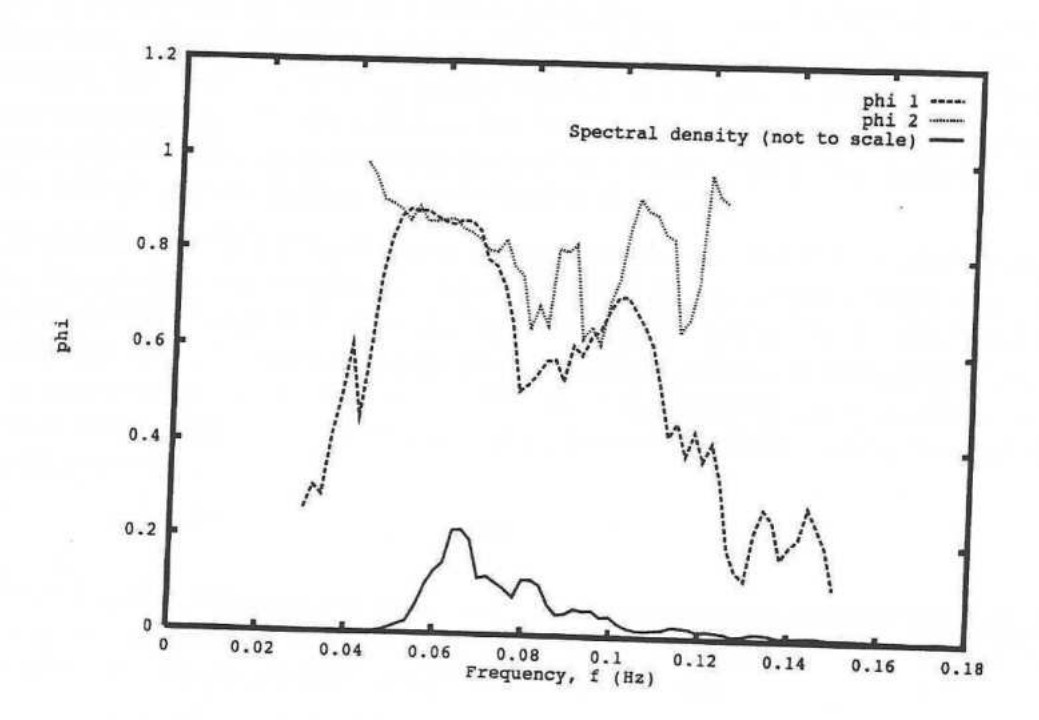


Fig. 6a. Directional spreading (ϕ) for hour 01:06 of storm 1992.

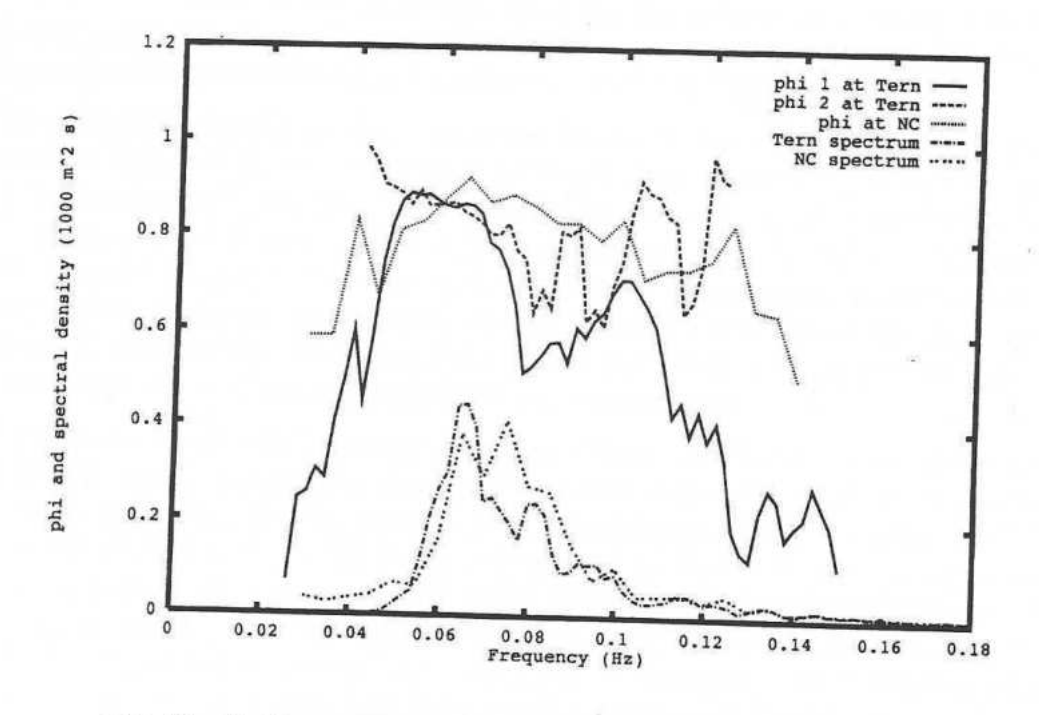


Fig. 6b. Surface spectra and spreading at Tern and North Cormorant

PROPERTIES OF INDIVIDUAL WAVES AND WAVE STATISTICS

For a narrow-banded Gaussian random process the crest and trough elevations are Rayleigh distributed (Rice, 1944-45; Longuet-Higgins, 1952). The real surface of the sea is broadbanded, this is reflected in the great variability in the crest amplitudes and local periods of successive waves. Also the surface is nonlinear, troughs and crests are of different shape, with the troughs being smaller and more rounded on average than crests. Both these effects should be visible in statistics derived from offshore measurements.

To second order in the wave slope, the dynamics of the underlying linear wave components are unaltered by the nonlinearity which produces bound waves at both sum and difference wavenumbers (Longuet-Higgins and Stewart, 1952; Taylor, 1992). We have used second order theory to transform measured crest and trough values into what they would have been if the second order effects were absent. Around a uni-directional crest located at (x=0,t=0), the linear surface can be described on average by the spatial correlation function scaled to the value at the crest

$$\eta(x,t=0) = \int_0^\infty d\omega \ a(\omega) \cos(kx),$$

where $a(\omega)$ is the (linear) amplitude spectrum of the extreme, which is the same shape as the power spectrum of the underlying random process. For waves on deep water (Taylor, 1992), second order nonlinear effects modify this surface shape to

$$\begin{array}{rcl} \eta(x,t=0) & = & \int_0^\infty d\omega \ a(\omega) \ cos(kx) \,.\, (1+\int_0^\omega d\omega' \,k \ a(\omega') \ cos(k'x) \,) \\ & - & \int_0^\infty d\omega \ k \, a(\omega) \ sin(kx) \,.\, \int_0^\omega d\omega' \ a(\omega') \, sin(k'x) \end{array} \,.$$

The double integrals reflect both the amplitude modulation and the horizontal transport of the short waves by the long waves. Thus, if non-linear crest and trough profiles with the same linear amplitude are averaged, the second order terms cancel. These expressions permit the conversion of the measured crest and trough values into the equivalent linear values, assuming that each of the crests and the troughs look like the correlation function. The linear spectral shape $a(\omega)$ is taken from the measured data as an hour-by-hour average. This is an acceptable approximation since the averaged spectrum is dominated by linear effects.

The probability density for the tails of the linearised crests and troughs are shown in Fig. 7 together with the density function for the Rayleigh distribution. The crest and trough values for all 3 storms (92, 93a, 93b) have been non-dimensionalised using the standard deviation of the surface elevation ($H_{s}/4$) within each hour and then combined into a single probability plot. The range of the plot corresponds to the largest 10% of the waves recorded over a total of 17 hours. Both measured distributions fit the Rayleigh curve (based on T_{z}) very well. Thus, standard linear theory can be used to estimate the statistics of the extreme waves so long as the trough-crest asymmetry is included using second order theory.

We have also examined the temporal history of large waves. For a linear model of the surface, it is now widely known that the most probable shape of a crest or trough is simply the correlation function for the random process (Lindgren, 1970; Boccotti, 1983; Tromans et al.,1991; Phillips et al., 1993). This is only exact for a narrow-banded process. However, for a large excursion the most probable shape tends to the correlation function, because the curvature and the surface elevation are increasingly correlated for larger waves. The use of the correlation function as a model for a design wave is discussed by Tromans et al.,1991, and it has been referred to in other publications from our group as NewWave.

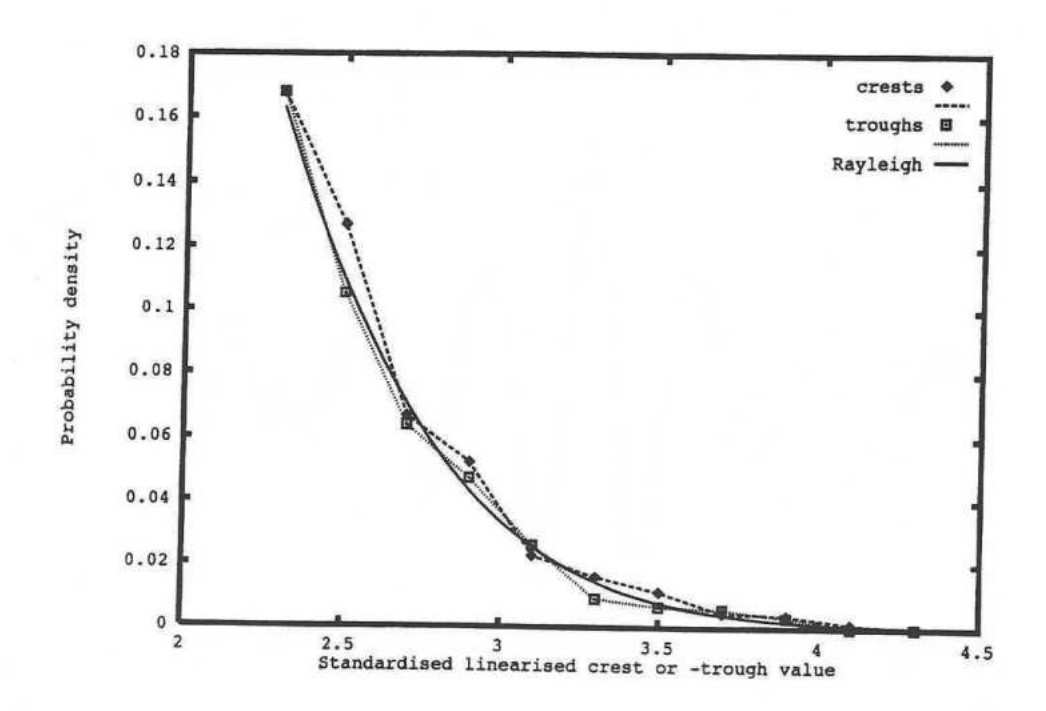


Fig. 7. Empirical p.d.f.s for linearised crests and troughs compared to Rayleigh.

For storm 93b, we have picked out crest and trough elevation data which contribute to a linear amplitude in the range 7.8-8.3m. Figure 8a shows the average time history of both crests and inverted troughs around the maximum. As predicted from 2nd order theory, the crests are higher and narrower and the troughs smaller and broader. The average value of the surface elevation drops to zero as the time shift from the extreme surface displacement increases. This rapid loss of coherence away from the maxima is characteristic of a broadbanded random process. Note also the average histories appear to be symmetric in time about the extreme value.

Figure 8b shows the local standard deviations of the surface elevations associated with the large crest or trough. These drop towards zero close to the maximum but relax further away towards the statistics of the random sea-state. The coherence imposed by picking large crests and troughs is only a local property for a broad-banded random process and the background variability of the underlying random process soon swamps the effect of conditioning on a large crest or trough. The non-stationary form of the variance (variability of the surface history away from the most probable) is described in Lindgren, 1970, Tromans et al.,1991 and Phillips et al., 1993.

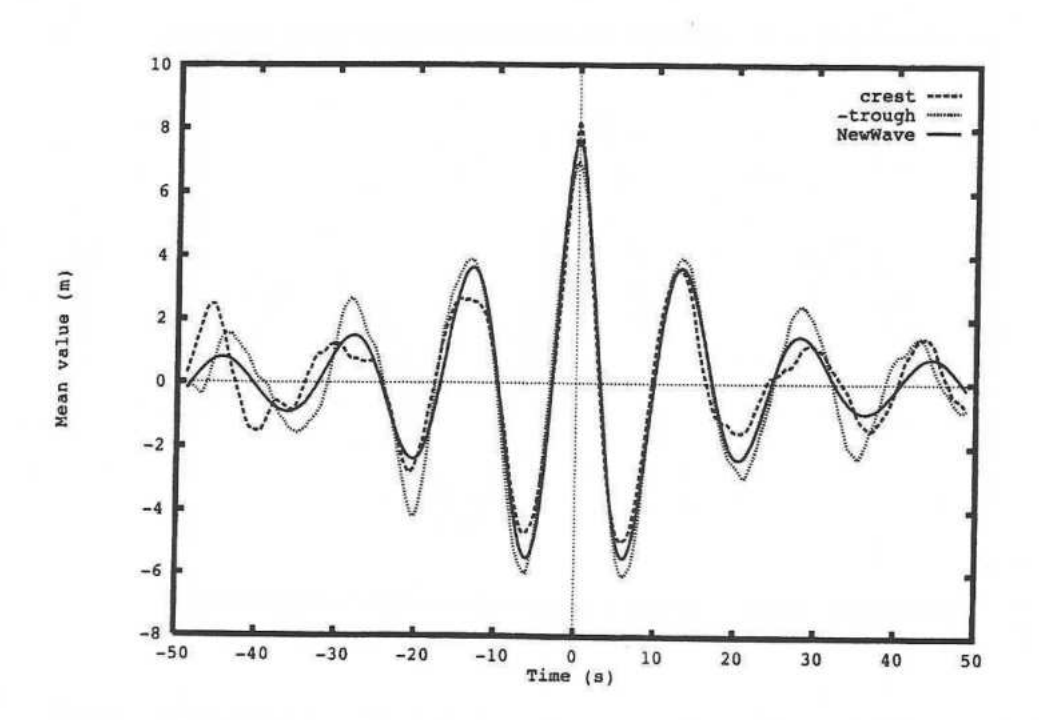


Fig. 8a. Averaged crest and trough time histories and the surface correlation (NewWave) for linearised extrema in the range (7.8m, 8.3m).

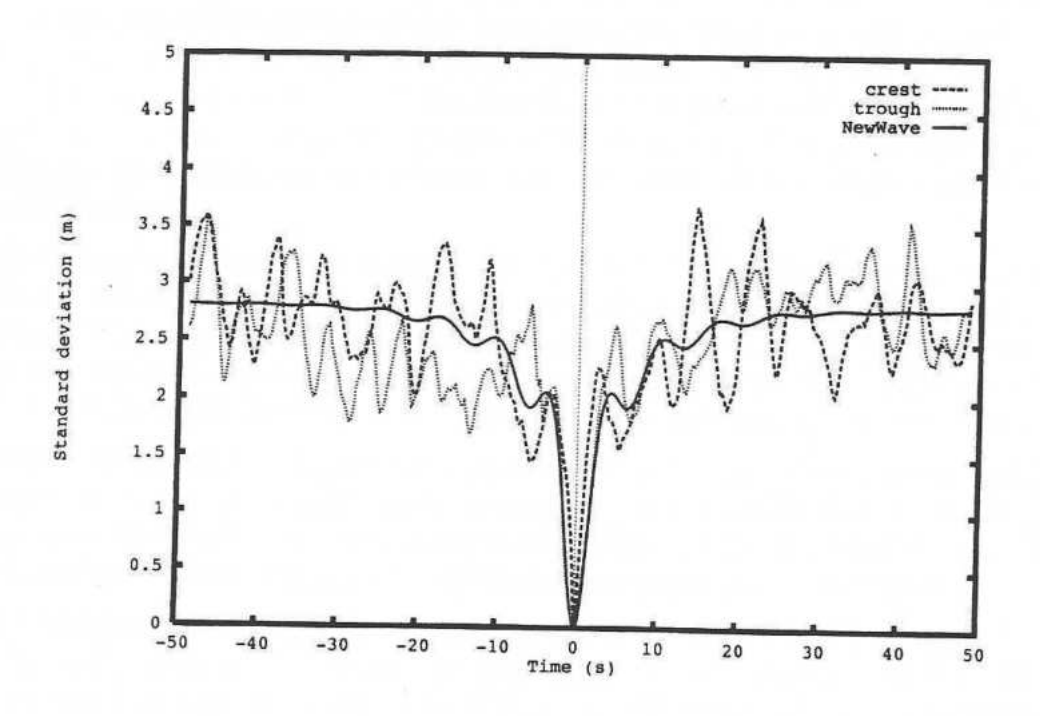


Fig. 8b. Standard deviations for crest and trough time histories compared to NewWave theory for linearised extrema in the range (7.8m, 8.3m).

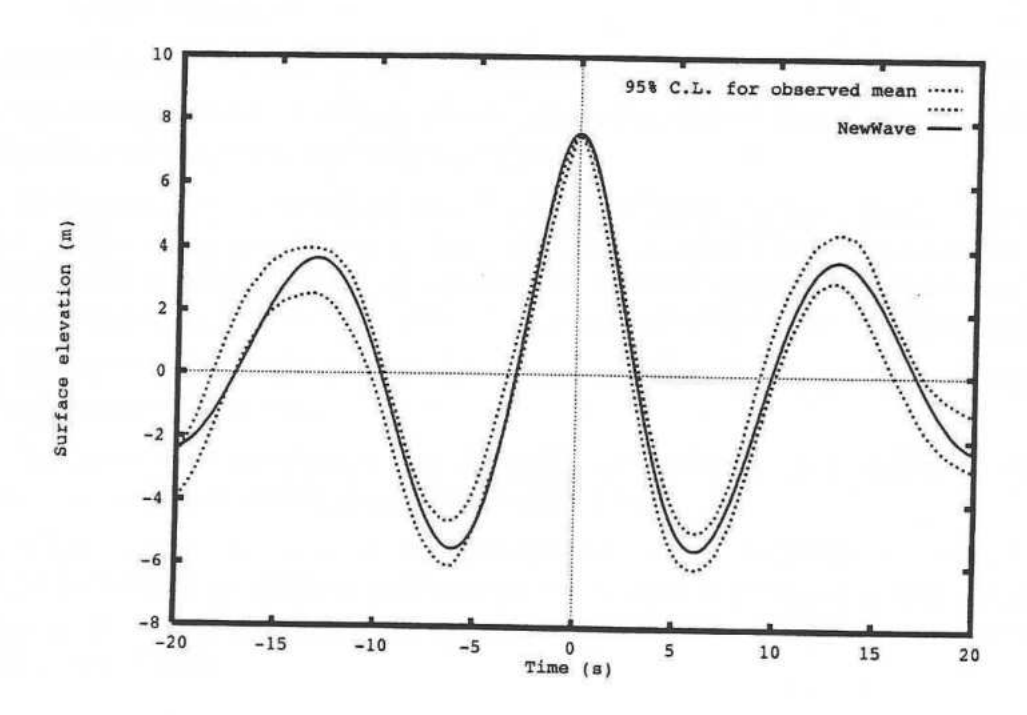


Fig. 9. 95% confidence band for the average of crest and inverted trough time history compared with NewWave.

If the crest and inverted trough time histories are added, the 2nd order terms cancel leaving only the linear profile and 3rd and higher order terms which may be negligible. The 95% confidence band for this averaged and linearised time history is shown in Fig. 9 together with the correlation function based on the averaged surface spectrum for this storm. Overall, the concordance between the correlation function and the measured data is good. Note though the width of the crest close to the maximum which is narrower than predicted using linear theory. Possibly this reflects the advection of high frequencies by low frequencies and higher order nonlinearities.

These results are similar to those of Phillips et al., 1993, who reported an analysis of buoy data. It is known, however, that buoys cannot be used to study the non-linearities of waves, because they move both horizontally and vertically (Tucker, 1991). We show that single point measurements, such as from the EMI laser wave-height meter, do record second-order effects. The magnitudes of these effects are approximately equal to those predicted by theory.

Overall these results suggest that, allowing for 2nd order effects, the underlying temporal structure of the wave field can be treated as Gaussian with local structure approximately matching the correlation function and extremes fitting a Rayleigh distribution. Modelling this wave environment using linear statistics therefore appears to be appropriate.

It should be noted that not all waves characteristics observed for North Sea storms are necessarily common to storms in other parts of the world. However, these offshore measurements support the approach adopted by Rodenbusch, 1986, for calculating wave loads on jacket structures in random sea-states, and further extended for full reliability analysis by van de Graaf, Tromans and Efthymiou, 1994.

CONCLUSIONS

Analysis of measured data for three severe storms in the northern North Sea shows

- 1. The ω^{-4} spectra tail previously observed by others and incorporated into model spectra by Donelan et al. is appropriate for these storms.
- 2. Wave spreading is minimized at a frequency below the spectral peak. The measurements made with fixed velocity meters on Tern have been analysed in two significantly different ways which yield virtually identical answers around the spectral peak. Even for the least spread frequency, the in-line velocity is reduced by a factor of 0.9 from the uni-directional value.
- 3. The crests and troughs in these storms are Rayleigh distributed, after accounting for the bound waves at 2nd order.
- 4. The linear correlation function for the surface elevation is a good model for the shape of a large wave, again after accounting for 2nd order effects.

Accurate models of the wave environment are crucial in Shell's approach to structural reliability analysis of offshore platforms under extreme storm loading. These results strongly support the idea of a design wave (such as NewWave) for modelling the extreme loading of offshore platforms.

Acknowledgement:

The authors are grateful to M. Efthymiou and I. Leggett of Shell Expro, G.Z. Forristall of SIPM and M. Kenley of Fugro McClelland for useful discussions and assistance.

REFERENCES

Boccotti P. (1983) Appl. Ocean Research 5, 134. 'Some new results on statistical properties of wind waves'.

Donelan M.A., Hamilton J. and Hui W.H. (1985) Phil. Trans. Roy.Soc.A 315, 509-562. 'Directional spectra of wind-generated waves'.

Forristall G.Z. (1981) Proceedings of the Conterence on Directional Wave Spectra Applications, ASCE, Berkeley, California, September 14-15 1981, 129-146. 'Kinematics of directional spread waves'.

Forristall G.Z., Ward E.G., Cardone V.J. and Borgman L.E. (1978) Jn. Phys. Oceanography 8, 888-909. 'The directional spectra and kinematics of surface gravity waves in tropical storm Delia'.

van de Graaf J.W., Tromans P.S. and Efthymiou M. (1994) OTC paper 7382, Proc 26th Annual Offshore Technology Conference (OTC), Houston. 'The reliability of offshore structures and its dependence on design code and environment'.

Lindgren G. (1970) Ann. Math. Statist. 41, 1870. 'Some properties of a normal process near a local maximum'.

Longuet-Higgins M.S. (1952) J. Marine Research 11, 266. 'On the statistical distribution of the heights of sea waves'.

Longuet-Higgins M.S. and Stewart R.W. (1964) Deep-Sea Research 11, 529-562. 'Radiation stresses in water waves: a physical discussion'.

Phillips O.M. (1993) 'Extreme waves and breaking wavelets' in Theoretical and Applied Mechanics 1992. Bodner S.R., Singer J., Solan A. and Hashin Z. (editors) Elsevier Science Publishers B.V.

Rice S.O. (1944-45) Bell System Technical Journal, 23, 282-332 and 24, 46-156. 'The mathematical analysis of random noise'.

Rodenbusch G. (1986) OTC paper 4098, Proc 18th Annual Offshore Technology Conference (OTC), Houston. 'Random directional wave forces on template offshore platforms'.

Taylor P.H. (1992) Proc. 6th International Conference on Behaviour of Offshore Structures (BOSS 92), Vol.1, 134-145. 'On the kinematics of large ocean waves'.

Tromans P.S., Anaturk A. and Hagemeijer P. (1991) 'A new model for the kinematics of large ocean waves - application as a design wave' in Proc. 1st International Offshore and Polar Engineering Conference, Edinburgh, Vol.3, 64-71.

Tucker M.J., 'Waves in Ocean Engineering - Measurement, Analysis and Interpretation', 1991. Ellis Horwood Ltd.

Wang D.W-C. (1992) Paper presented at ISOPE-92-C5-78 'Estimation of wave directional spreading in high seas'.